Effects of Phase Separation on Structural Characteristics of Poly(vinyl chloride) Physical Gels

Po-Da Hong* and Che-Min Chou

Department of Fiber and Polymer Engineering, National Taiwan University of Science and Technology, Taipei, 10607, Taiwan

Received June 30, 2000; Revised Manuscript Received October 14, 2000

ABSTRACT: The effects of phase separation on structural characteristics of poly(vinyl chloride)/chlorobenzene (PVC/ClBz) physical gels were studied through the time-resolved light scattering, pulsed NMR, and the gelation kinetic analyses. The present study clarifies the characteristics of PVC solutions at various concentration regions and their influence on the gel structure formed from the spinodal decomposition of the solutions. According to the physical meaning of the $[\eta]C$ value capable of expressing the characteristics of PVC solutions, one can divide the chain aggregation behaviors into four regions with increasing PVC concentration. (1) At the concentration less than the macroscopic percolation transition limit, the polymer-rich phase transforms into isolated droplets, and the gelation cannot occur. (2) When the concentration is close to the critical gelation concentration C^*_{gel} (ca. $[\eta]C \sim 1.5$), the gelation behavior depends on the competition between transitions of the sol−gel type and the dynamic percolation-to-cluster type; moreover, the structure and properties of gels are mainly dominated by the evolution of the later-stage phase separation. (3) At the concentration exists between the C^*_{gel} and the chain overlapped concentration C^* (ca. $[\eta]C \sim 4$), the initial stage phase separation controls mainly the structural formation of PVC gels. (4) As the concentration is further increased more than $[\eta]C \sim 4$, i.e., the overlapping between chains coils is present in this region, the influence of phase separation on PVC/ClBz gelation would be weakened. It should be noted that the C^* value is higher than the C^*_{gel} value in this work, implying that the chain overlapping is not a prerequisite for the gelation of PVC solutions to undergo liquid−liquid phase separation. Thus, the aggregation behavior of PVC solutions in region 3 was focused in order to emphasize the effect of initial phase separation on gelation. As a result, the gelation mechanism and the structural characteristics of PVC gels can be interpreted well by our proposed model.

Introduction

Thermoreversible physical gel is a three-dimensional network of polymer chains cross-linked by physical association. Basically, the gelation behavior of polymer solution can be affected by many factors such as temperature, concentration of polymer, and type of solvent used.[1−5] Therefore, the associated kinetic and thermodynamic studies regarding how the structure forms during gelation is of great interest to researchers. Generally, there are three fundamental mechanisms to be considered for the gelation behavior, i.e., the liquid−liquid phase separation by spinodal decomposition,[6,7] the liquid−solid phase transformation by crystallite formation of the polymer chain segments,[8,9] and the percolation model (a statistical mechanical model of sol−gel transition).[10,11] However, the mechanisms involved with structural formation for polymer physical gels are very complex, resulting in difficulties to elucidate fully in terms of the gelation phenomena.

The analysis of gelation kinetics is one of the most important aspects of understanding the macroscopic mechanism of gelation. As far as the percolation theory[11] is concerned, the gel fraction, G, which is the ratio of the molecular content in a gel macromolecule to that in the total molecular content, can be expressed by

$$G \propto (p - p_c)^{\beta} \tag{1}$$

where p is the conversion factor, i.e., the ratio of the actual number of bonds at any given moment to the greatest possible number of such bonds in the three-dimensional lattice, p_c is the critical conversion factor required for gelation, and β is a critical exponent ($\beta = 0.45$ for a three-dimensional lattice model). Recently, according to the aspect of chemical kinetics, Mal et al.[12] have expressed that the gel fraction is proportional to the gelation rate, and it was used as a satisfactory lattice percolation model to explain the gelation rate of poly(vinylidene fluoride) physical gels. However, it is necessary to mention that this model developed for polyfunctional condensation of monomers is not the keystone to the success of physical gelation of polymer solution, although the experimental results obtained from this approach clearly support this lattice percolation model. Surprisingly, we have obtained further understanding of polymer gelation by using the concept of percolation model to develop a clear structural model to be applied to the physical gelation of polymer solution. In other words, it has been demonstrated in this paper that the percolation-type association for polymer gelation is the consequence of intermolecular aggregation between chain coils in a phase separation process.

With various scattering techniques Takeshita et al.[13] have already proposed a good model for the hierarchic structure of poly(vinyl alcohol) gel from the spinodal decomposition of the solution. Moreover, they qualitatively explained a possible mechanism of the gelation process for PVA solution under spinodal decomposition.[14] However, they have not proposed a complete and clear structural model for understanding the effect of phase separation on structural formation and characteristics of physical gels. In our previous paper,[5] it is

* Corresponding author. Tel +886-2-27376539, Fax +886-2-27376544, E-mail phong@hp730.tx.ntust.edu.tw.

10.1021/ma0011439 CCC: $19.00
Published on Web 12/01/2000

illustrated from the thermodynamic and kinetic point of view that the essential effects of having crystallization and phase separation on the gelation of poly(vinylidene fluoride)/tetra(ethylene glycol) dimethyl ether solutions. Concurrently, it is clarified that the gelation when occurred in a phase separation system can be divided into two regions by a kinetic transition concentration, C^*_{tran}. As the low concentration solution undergoes spinodal decomposition, the phase separation is the rate-determining step for gelation. Meanwhile, the crystalline nucleation is the rate-determining step for the high concentration one, indicating that the influence of phase separation on gelation behavior may have been weakened. Similarly, the kinetics of spinodal decomposition in phase-separating systems must dominate the morphology, structure, and properties of the gels,[15,16] especially in the low-concentration region. Therefore, the gelation mechanism and its dependence on thermodynamics, i.e., the temperature, and on kinetics, i.e., the concentration, should be discussed in detail, and the relation between the phase separation, gelation behaviors of polymer solution, and network structure should be clarified.

In this work, we first clarified the characteristics of PVC solutions at various concentration regions and their influence on the structural formation of gels from spinodal decomposition process. Then initial phase separation of the solution was discussed as well to highlight its effect on structural formation of gels. Finally, we shall explain the process of gelation and the corresponding characteristics of hierarchic structure using our proposed model.

Experimental Section

Materials. Poly(vinyl chloride) (PVC) powder ($\bar{M}_w = 2.33 \times 10^5$, Aldrich Chemical Co.) was used in this experiment. The polydispersity index ($\bar{M}_w/\bar{M}_n = 1.94$) was determined from GPC measurement of a 0.5 g/dL tetrahydrofuran solution of PVC. The solvent, chlorobenzene (ClBz), was filtered by using 0.02 μm Teflon filter (Whatman International Ltd, England: Anotop 25 plus syringe filter) for removing dust. The homogeneous PVC solutions were prepared by dissolving the PVC powder at 130 °C in sealed test tubes and then quenched to the ambient temperature for measurements.

Gelation Rate. First, PVC solutions with various concentrations containing in sealed test tubes (8 mm i.d. and 10 cm in height) were kept in an oven at 130 °C for about 1 h to make the solutions homogeneous before measurements. Then the hot solutions were quickly transferred into water bath being kept at a given temperature to be controlled within ±0.1 °C. The test tube tilting method was used for determining the gelation time (t_{gel}), which was defined by observing cessation of the liquid flow inside the test tube when it was tilted, and the gelation time was monitored just after the test tube was put into the thermostatic bath. The reciprocal of gelation time of the solution is defined as the apparent gelation rate, t_{gel}^{-1}.

Intrinsic Viscosity. The determination of the viscosity of dilute PVC solution was carried out using an Ubbelohde viscometer immersed in a thermostatic water bath to be held at 30 ± 0.1 °C for 1 h. The intrinsic viscosity, [η], was obtained by the Huggins equation:[17]

$$\frac{t - t_0}{t_0 C} = \frac{\eta_{sp}}{C} = [\eta] + k'[\eta]^2 C \qquad (2)$$

where t is the flow time of the dilute solution, t_0 the flow time of the pure solvent, C the concentration of polymer, η_{sp} specific viscosity, and k' the Huggins constant.

Time-Resolved Light Scattering. The measurement was carried out using a Malvern series 4700 apparatus with the light source being a 25 mW He−Ne laser. In addition, a vertically polarized light having a wavelength of 633 nm was focused on the sample cell through a temperature-controlled chamber (the temperature being controlled to within ±0.1 °C) filled with distilled water. The hot homogeneous solutions were quickly quenched in the temperature-controlled chamber at constant temperature. The time dependence of scattered intensity during the isothermal phase was measured using the step scattering measurement within the scattering vector (q) range between 2.012×10^{-5} and 2.674×10^{-5} cm^{-1} [$q = (4\pi n/\lambda)\sin(\theta/2)$, where θ is the scattering angle, n is the refractive index of the medium, and λ is the wavelength of incident light]. In this work, the light scattering measurement was carried out by rotating the test tube to reduce the effect of sample's inhomogeneity.

Pulsed ^{1}H NMR. The measurement was performed by a MARAN-20 pulsed NMR spectrometer operating at a fixed frequency 20 MHz. The recovery time of the spectrometer following a sequence of pulse was 10 μs. The spin−spin relaxation time, T_2, was determined by the Carr−Purcell−Meiboom−Gill (CPMG) method[18] [$90°_x\tau(180°_y2\tau)_n$](τ = 50 μs, $P90°$ = 2.9 μs,n = 4096) to eliminate the effect of the heterogeneity in the static magnetic field. The CPMG pulsed sequence was available for the long T_2 samples, e.g., the wet gels.

To analyze NMR's decaying signals**,** the Weibull function was used to express the decay of the transverse magnetization intensity, $M(t)$.[19,20]

$$M(t) = M_0 \exp[-(1/a)(t/T_2)^a] \qquad (3)$$

where M_0 is a constant proportional to the total number of the nuclei with magnetic moment, T_2 is the transverse relaxation time, and t is the decay time. The a factors are the shape parameters, which could be disposed to become a hard (immobile) component and a soft (mobile) component for a = 2 (Gaussian decay) and a = 1 (exponential decay), respectively. As the heterogeneous gel led to the heterogeneity on the molecular motion, the CPMG signals could be decomposed into several decaying components with various T_2 values, as shown in eq 4.

$$M(t) = \sum M_0^i \exp[-(1/a)(t/T_2{}^i)^a] \qquad (4)$$

where M_0^i is the magnetic moment fraction of ith component.

Results and Discussion

Kinetics of Gelation. The analysis of gelation kinetics is an important step to understand the gelation mechanism, and it is usually done through the analysis of the apparent gelation rate. The apparent gelation rate can be obtained from the reciprocal of gelation time, t_{gel}, which is the time required for the polymer solution to form the gel. Figure 1a shows the t_{gel}^{-1} values of the PVC/ClBz solutions as a function of polymer concentration at various gelation temperatures. The result shows that the t_{gel}^{-1} increases with increasing concentration and increases with decreasing temperature. To determine the critical concentration of gelation, C^*_{gel}, all curves in Figure 1a were extrapolated to zero gelation rate. The C^*_{gel} values at 30 and 40 °C are about 1.9 and 2.1 g dL^{-1}, respectively. Generally, the gelation rate can be conveniently expressed as a function of concentration. To provide a general description of the concentration function, the reduced concentration and the exponent n should be introduced. Therefore, at a given temperature the gelation rate is expressed as a general relationship by[12,21,22]

$$t_{gel}^{-1} \propto \left[\frac{C - C_{gel}^*}{C_{gel}^*}\right]^n \quad (5)$$

where n is exponent value depending on the gelation mechanism. Figure 1b shows the double-logarithmic plots of t_{gel}^{-1} as a function of reduced concentration at various gelation temperatures. From the slope it can be seen that the n value is very close to 0.45 for the percolation exponent β in a three-dimensional lattice model.[11] In this work, the exponent values are quite different from those in our previous study for the gelation of PVDF/TG solutions; i.e., the exponent value is "2" for bimolecular association in the cross-link process[5,22] and "1" for the diffusion of polymer chains in the phase separation process. The n value of 0.45 is similar to that reported by Nandi et al.[12,21] for the study of PVDF gels. To understand the relation between the kinetic exponent "n" and the corresponding gelation mechanisms, we may consider that the gelation process exists a competitive situation of these phenomena as stated above. For PVC/ClBz solutions, the gelation depends on the formation of three-dimensional percolation structure, implying that the gelation may be related to the phase transition after the collection of finite clusters to become an infinitely large network structure.

Generally, the gelation of polymer solution should take place beyond the chain overlapping concentration C^*. On the other hand, the intrinsic viscosity $[\eta]$ is a characteristic function of the single polymer chain in a solution. Intuitively, the intrinsic viscosity can aptly reflect the effective hydrodynamic volume of the polymer chain in a solution because of its unit.[23] Hence, Frisch and Simha[24] suggested that the dynamic behavior of polymer solution could be classified into several regions using the semiempirical rule based on the interaction degree between polymer chains. In the infinite dilution limit, which is defined as a concentration below $[\eta]C \sim 1$, the polymer chain acts as an isolated coil. If the concentration of polymer in a solution is raised, the hydrodynamic screening limit will be reached, and the relative proximity of neighboring chains allows polymer−polymer intermolecular interactions to influence the motion of the polymer chains. Perturbation of the polymer motion by this mechanism is expected to occur above a concentration as defined by $[\eta]C > 1$. The effect may be expected to be cumulative up to the concentration corresponding to the chain overlapping concentration, where the close packing of polymer coils in solution exists at the concentration of $[\eta]C \sim 4$. Once the overlapping concentration is attained, the polymer motion will be dominated by the presence of direct polymer−polymer interactions. If the increasing concentration rises beyond the limit of $[\eta]C \sim 10$, the interpenetration of the polymer coils or the pseudo-matrix-gel will be formed. To obtain more detailed information on the characteristics of the PVC/ClBz solution over a wide concentration regime, the $[\eta]C$ value could be employed as a simple, approximate, and overlap criterion to express the aggregation behavior of polymer solutions.

Figure 2a shows the η_{sp}/C versus C for PVC/ClBz solution at 30 °C. From the linear relationship in Figure 2a, the $[\eta]$ value can be obtained from the intercept of η_{sp}/C at $C = 0$. According to the semiempirical rules proposed by Frish and Simha, Figure 2b shows the apparent gelation rate as a function of the $[\eta]C$ value

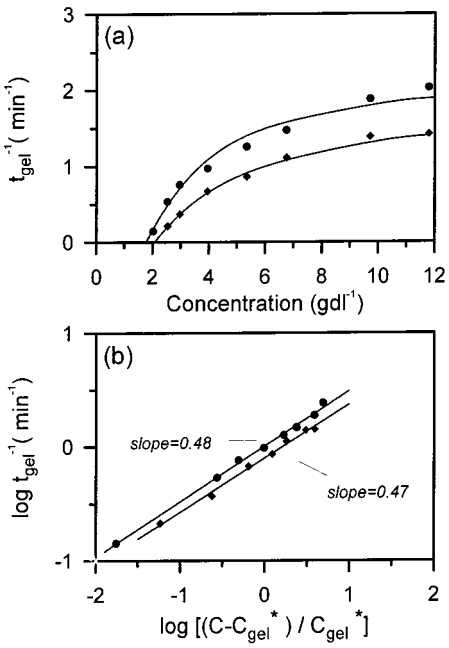

Figure 1. (a) Apparent gelation rate, t_{gel}^{-1}, as a function of concentrations. (b) log t_{gel}^{-1} versus log$[(C - C_{gel}^*)/C_{gel}^*]$ plot for PVC/ClBz solutions at various temperatures: (●) 30 °C; (◆) 40 °C.

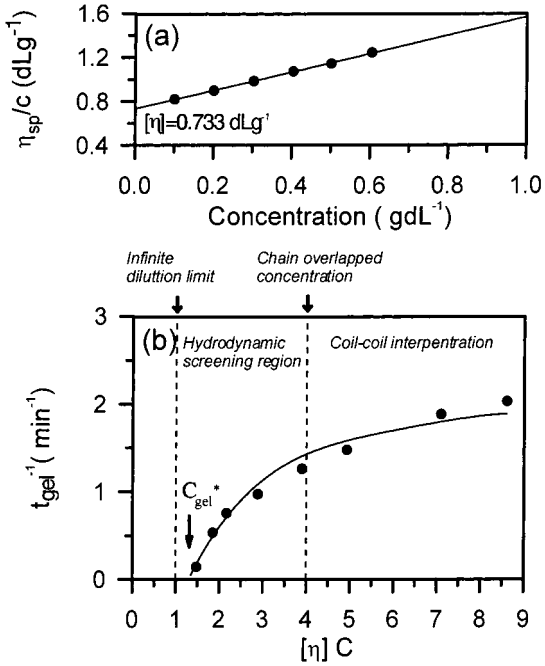

Figure 2. (a) Plot of the η_{sp}/C versus C for PVC/ClBz dilute solution. (b) Apparent gelation rate, t_{gel}^{-1} versus $[\eta]C$ at 30 °C.

at 30 °C. Some distinct features can be seen to be dependent on the $[\eta]C$ value. At the concentration below $[\eta]C \sim 1$, i.e., an infinite dilution region, the gelation will not happen. The gel formation occurs in the concentration region of $1 < [\eta]C < 4$, where the concentration range is located within the hydrodynamic screening region. In this region, the polymer−polymer intermolecular interactions will begin to affect the aggregation behavior of polymer chains in solution, and the apparent gelation rate rises rapidly with the increasing concentration. However, it should be noted that the polymer solution does not reach the chain overlap-

ping concentration, C^*, in this region. As the concentration increases beyond the C^* (ca. $[\eta]C \sim 4$), the polymer coils start to overlap, and the apparent gelation rate is almost independent of the concentration. Ohkura et al.[25] studied the gelation of PVA in a DMSO/water mixture and pointed out that the homogeneous solution at the concentration less than C^* could not form a gel, because the cross-linking points were not capable of connecting among themselves across the whole system. Therefore, the chain overlapping is a prerequisite to gelation for homogeneous solution. In this study, the chain-overlapped concept concluded in the gelation of PVC/ClBz solutions was invalid, because the gelation may occur in a heterogeneous solution system. In other words, the liquid−liquid phase separation or spinodal decomposition may strongly affect the structural formation of PVC gels.

Spinodal Decomposition. The phase separation of PVC/ClBz solution can be described by the linear theory of spinodal decomposition which has been applied to some physical gelation systems,[5−7] if the gelation behavior is related deeply with phase separation as discussed above. In fact, the spinodal decomposition at the initial stage of phase separation should be described well using Cahn's linear theory.[26,27] The scattered intensity is given as follows:

$$I(q,t) = I(q,t=0)\exp[2R(q)t] \tag{6}$$

where $I(q,t)$ is the scattered intensity at a given scattered vector q and time t. The $R(q)$ value being the growth rate of concentration fluctuation is given by

$$R(q) = D_c q^2\left\{-\frac{\partial^2 f}{\partial C^2} - 2\kappa q^2\right\} \tag{7}$$

where D_c is the cooperative diffusion coefficient of polymer chains in solution, f is the free energy of mixing, C is the concentration of solution, and κ is the concentration-gradient energy coefficient defined by Cahn. According to eq 6, the exponential increase in scattered intensity with time can be described by a linear theory. Figure 3 shows the change with respect to logarithm in terms of the scattered intensity as a function of time at various scattering vectors for 3.9 g dL^{-1} PVC/ClBz solution at 30 °C. First, the scattered intensity increases exponentially and then deviates from the exponential relationship with the lapse of time. From Figure 3, the slope of the straight line with its number being derived from eq 6 as $2R(q)$ can be used to estimate the concentration of fluctuation rate $R(q)$ at a given value q. Linear results were also obtained for other solutions at various concentrations and temperatures.

Figure 4 shows the result of $R(q)/q^2$ as a function of q^2 for 3.9 g dL^{-1} PVC/ClBz solution at various temperatures, contributing to fairly good linear relationships. From these plots along with eq 7, one can estimate the following characteristic parameters used to describe the dynamics of phase separation: (1) such as the apparent diffusion coefficient $D_{app} = -D_c(\partial^2 f/\partial C^2)$ from the intercept of $R(q)/q^2$ at $q = 0$, (2) the most probable wavenumber of fluctuations, q_c, which can grow from the intercept of q^2 at $R(q)/q^2$ at $q = 0$, and (3) the most probable wavenumber of fluctuations that can grow at the highest rate to be estimated from $q_m = q_c/2^{1/2}$. The calculated parameters are summarized and shown in Table 1. Practically, in Figure 3 the q_m, which the growth of scattered intensity is maximal in the early

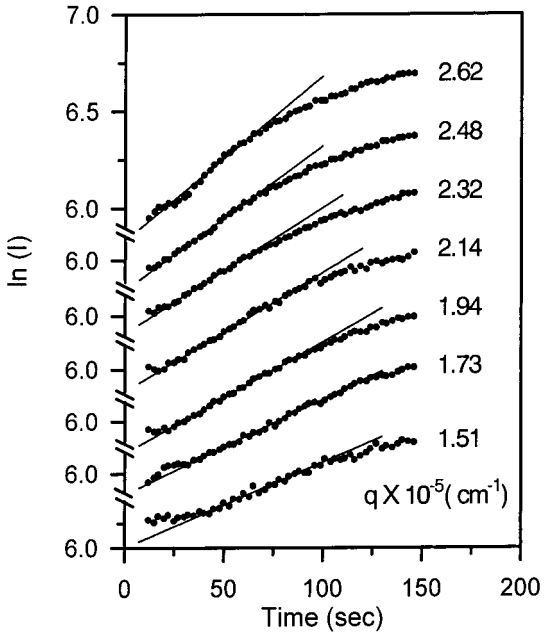

Figure 3. Time evolution of the logarithm of scattered intensity at various q for 3.9 g dL^{-1} PVC/ClBz solution at 30 °C.

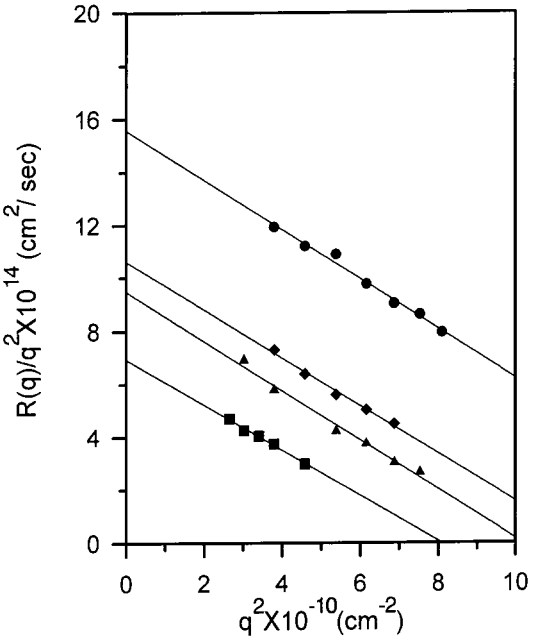

Figure 4. Plot of $R(q)/q^2$ versus q^2 for 3.9 g dL^{-1} PVC/ClBz solution at various temperatures: (●) 30 °C; (◆) 35 °C; (▲) 38 °C; (■) 40 °C.

stage of phase separation, exists outside the measuring region at this concentration and temperature conditions. Therefore, the q_m cannot be directly observed. To check such spinodal decomposition, the $R(q)$ value was plotted as a function of q at various temperatures, as is shown in Figure 5. The result clearly showed a peak in the plot except the result at 30 °C. Besides, the experimental q_m values correspond well to the calculated values from the plot of $R(q)/q^2$ vs q^2. This fact directly indicates that the phase separation behavior of PVC/ClBz solutions could be described using Cahn's theory. Figure 6 shows the temperature dependence of D_{app} value at various concentrations. The spinodal temperature T_s can be obtained with D_{app} equal to zero from the intercept on

Table 1. Characteristic Parameters Describing Spinodal Decomposition of PVC/ClBz Solution

concn (g/dL)	$[\eta]C$	T (°C)	$D_{app} \times 10^{14}$ (cm^2/s)	$q_c \times 10^{-5}$ (cm^{-1})	$q_m \times 10^{-5}$ (cm^{-1})	$\Lambda m^a \times 10^5$ (cm)	T_s (°C)
2.0	1.5	30	20.26	2.75	1.94	3.23	
2.5	1.8	30	13.60	3.35	2.37	2.65	50.7
		35	10.62	3.12	2.20	2.86	
		38	8.69	2.59	1.83	3.43	
		40	6.82	2.42	1.71	3.67	
2.9	2.1	30	16.32	3.54	2.50	2.51	51.3
		35	12.00	3.09	2.18	2.88	
		38	9.68	2.88	2.04	3.08	
		40	8.72	2.57	1.82	3.45	
3.9	2.9	30	13.93	3.98	2.82	2.23	51.8
		35	10.61	3.42	2.42	2.59	
		38	9.48	3.18	2.26	2.78	
		40	6.94	2.84	2.01	3.13	
5.4	3.9	30	18.29	4.02	2.84	2.21	53.4
		35	13.95	3.71	2.62	2.39	
		38	11.68	3.35	2.37	2.65	
		40	9.69	3.23	2.29	2.74	

[a] The characteristic dimension of concentration fluctuation, $\Lambda_m = 2\pi/q_m$.

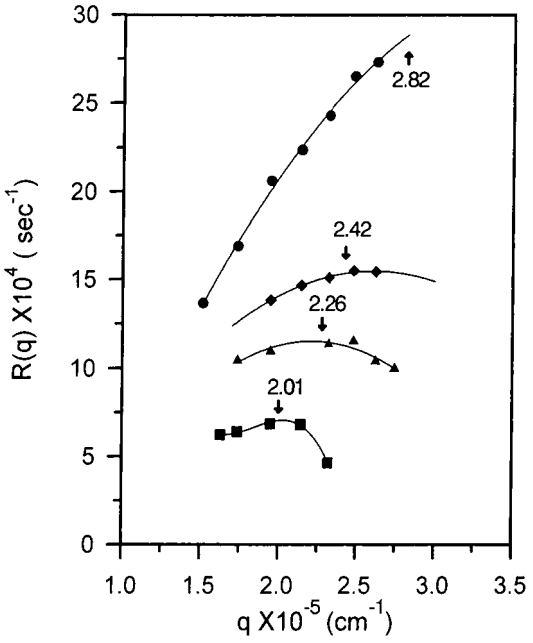

Figure 5. Variation of growth rate $R(q)$ of spinodal decomposition with q measured for 3.9 g dL^{-1} PVC/ClBz solutions at various temperatures: (●) 30 °C; (◆) 35 °C; (▲) 38 °C; (■) 40 °C.

the temperature axis using Figure 6, and this result is shown in Table 1 as well.

To obtain more detailed information on the gelation characteristics, the relationship between the phase separation and the gelation time is discussed. Figure 7 shows the relationship between the phase separation and gelation for PVC solutions with various concentrations at 30 °C. The data at the initial stage of each phase separation demonstrate that there exists an exponential increase in the scattered intensity with respect to time at various concentrations. As time is increased, the scattered intensity deviates from the exponential relationship. Comparing the results with the gelation kinetics, this deviation can be attributed to the gel formation except for the solution with the lowest concentration ($[\eta]C = 1.5$). In concentration regions $[\eta]C > 1.5$, the gelation takes place immediately after the initial phase separation. Since the phase separation does not go through intermediate or later stage's spinodal decomposition, the characteristics of percolating structure at its early stage are pinned due to the onset of gelation. This also indicates that the phase separation at the initial stage controls the gel morphology mainly and thus makes a direct impact on the structure and properties of the gels in these concentration regions. Regarding the concentration at $[\eta]C = 1.5$, which is close to the critical gelation concentration C^*_{gel}, the gelation occurs after the initial phase separation. In other words, the gel starts its formation process beyond the time frame of spinodal decomposition period, i.e., from the exponential growth at the early stage to intermediate or later stages. Hence, the deviation of scattered intensity from the exponential relationship is considered to

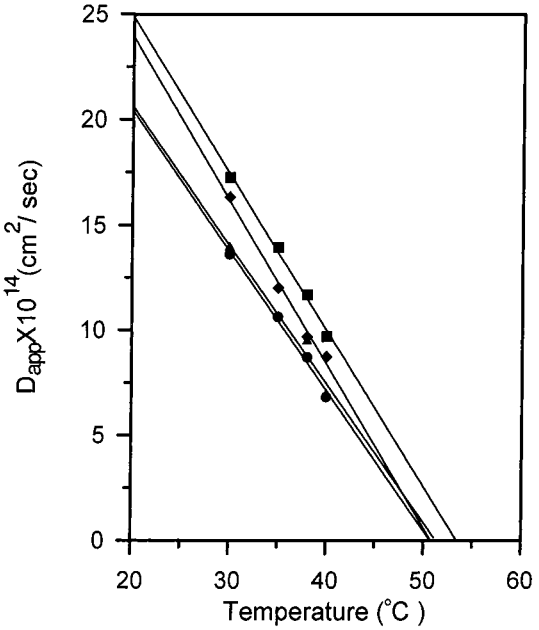

Figure 6. Temperature dependence of the apparent diffusion coefficient, D_{app}, at various concentrations: (●) 2.5 g dL^{-1}; (◆) 2.9 g dL^{-1}; (▲) 3.9 g dL^{-1}; (■) 5.4 g dL^{-1}.

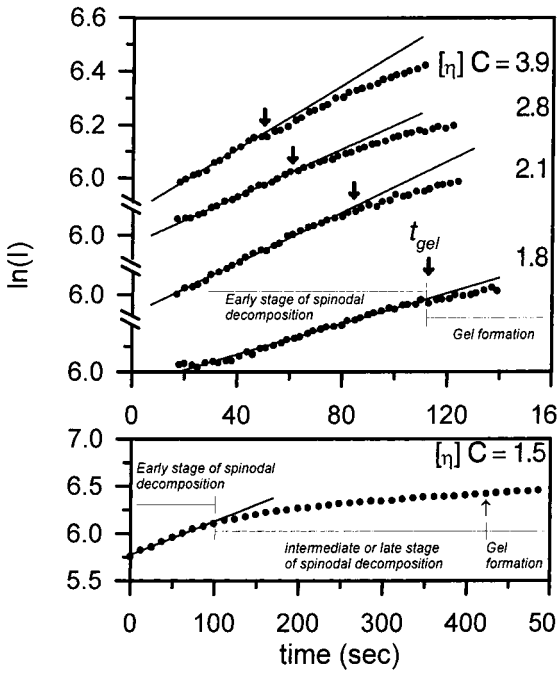

Figure 7. Relationship between the phase separation and gelation behaviors for various concentrations at 30 °C.

be attributable to a consequence of coarsening effect at the later stage of spinodal decomposition. From the viewpoint of structural design we believe that the morphological development relating to the later stage of spinodal decomposition is crucial to the structural formation of gels at the concentration close to C^*_{gel}. With this we believe that there are two effects related to the gelation at the concentration near the C^*_{gel}: (1) the structure and properties of the gels should be concerned with the development of the phase separation domain structure in later stage's spinodal decomposition, and (2) the formation of three-dimensional network structure strongly depends on whether the dynamical percolation-to-cluster transition takes place or not. This transition during the coarsening process of spinodal decomposition has been suggested by Hasegawas et al.[28] from their study on phase separation behavior of the polymer blend. However, the quantitative investigation of the kinetic competition between the gelation and dynamic percolation-to-cluster transition is very complex. Up to now, the critical gelation phenomena have not been fully elucidated. Studies on this critical gelation region require further works including both theories and experimentation. In this article, we focus only on the effects that are related to spinodal decomposition at early stage in gelation.

As mentioned above, the phase separation process at the initial stage within the $1.5 < [\eta]C < 4$ region controls the morphology of gels. The characteristic of percolating structure at the initial spinodal decomposition is restrained due to the onset of gelation. Hence, at the initial spinodal decomposition process, the characteristic size of the phase separation domain, $\Lambda_m = 2\pi/q_m$, is the most important parameter used to describe the structural characteristics of gels in terms of the spacing between polymer-rich regions. From Table 1, the characteristic size, Λ_m, seems to be dependent on concentration and temperature simultaneously. According to the theory concerning spinodal decomposition of polymer solution proposed by Van Aartsen,[29] the characteristic fluctuation wavelength, Λ_m, is theoretically given by

$$\Lambda_m = 2\pi\xi\left[3\left(1 - \frac{T}{T_s}\right)\right]^{-1/2} \qquad (8)$$

where ξ is the range of molecular interaction, and T and T_s are the experimental and spinodal temperatures, respectively. Equation 8 expresses that the Λ_m value decreased with the increasing of the difference between the experimental and spinodal temperatures if the range of molecular interaction is independent of temperature. This theory is rather reasonable in very concentrated solutions, because it used the Flory–Huggins relationship to express the free energy of mixing (the mean-field approximation). In contrast, Van Aartsen's equation does not hold in the dilute concentration region since the fluctuation effects are too large and the mean-field approximation tends to break down. For this reason we consider such a solution to be a more or less homogeneous system as $[\eta]C > 1$. It may be still possible to use this relationship to discuss the characteristic size of the phase separation domain. Figure 8a shows the Λ_m value as a function of $[3(1 - T/T_s)]^{-1/2}$. Fairly good linear relationships were obtained, and the Λ_m value will be zero at spinodal temperature. From the plot and eq 8 the ξ value obtained from the slope of straight line in Figure 8a is shown in Figure 8b. The ξ

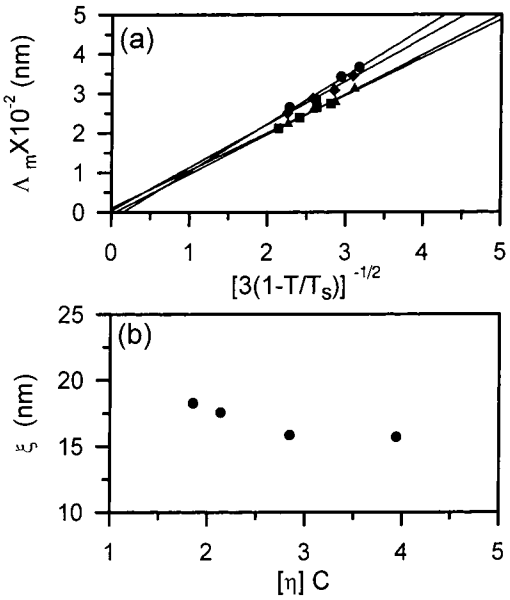

Figure 8. (a) Relationship of Λ_m as a function of $[3(1 - T/T_s)]^{-1/2}$ based upon the Van Aartsen's theory at various concentrations: (●) 2.5 g dL^{-1}; (◆) 2.9 g dL^{-1}; (▲) 3.9 g dL^{-1}; (■) 5.4 g dL^{-1}. (b) The range of molecular interaction, ξ, versus $[\eta]C$.

value varies slightly from 18.3 to 15.7 nm with increasing concentration. On the basis of the study of critical opalescence in polymer solution, Debye[30−32] suggested that the range of molecular interaction's value should be equal to the radius of gyration of polymer chain, assuming that the segment density of polymer coil follows a Gaussian distribution. Comparing the ξ value with the size of chain coil reported in our previous paper,[3] this value is very close to the hydrodynamic radius of PVC coil in dilute solution. Although the hydrodynamic radius primarily reflects the hydrodynamic behavior of the polymer coil, the value of ξ depends on the thermodynamic quality. However, it is sufficient to fully relate the actual meaning of interaction range. Therefore, it directly indicates that the range of molecular interaction corresponds, at least in the order of magnitude, to the average distance between the polymer coils in such a solution. This may also imply that the intermolecular associations between chain coils play an important role in the initial concentration fluctuation.

On the other hand, Van Aartsen pointed out that the ξ value would depend on the thermodynamic quality of the solvent, temperature, and most probably on the concentration. The last point is especially important in the rather concentrated solutions. When the polymer concentration is increased beyond the C^* ($[\eta]C = 4$) where the coils start to overlap with each other, we may expect that the range of molecular interaction would proportional to the mesh size or correlation length. Then these phenomena can be expressed by a certain scaling relationship between the range of molecular interaction and concentration. However, in the present system it is very difficult to quantitatively explain the concentration dependence of the ξ value, because the gelation rate is so fast to interfere with spinodal decomposition process as the increasing concentration rises beyond the $[\eta]C \sim 4$ limit. Nevertheless, we could still qualitatively explain the structural characterization of gels formed at the $1.5 < [\eta]C < 4$ region through the characteristic

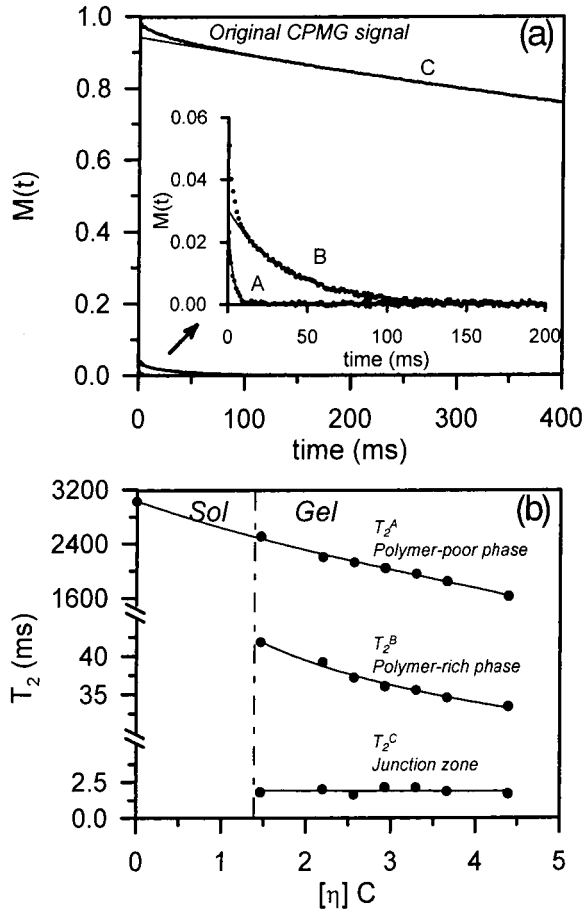

Figure 9. (a) CPMG decaying signals of 5 g dL^{-1} PVC/ClBz gel at 30 °C. (b) Spin−spin relaxation time T_2 of each component as a function of $[\eta]C$.

fluctuation wavelength and the range of molecular interaction simultaneously.

Pulsed NMR Analyses. Recently, the heterogeneous structures of multicomponent polymer systems (e.g., polymer gels, polymer blends, and polymer solutions) have been studied through pulsed NMR measurements.[4,33−36] The decaying signals of heterogeneous materials in pulsed NMR measurement can be decomposed into various components having different relaxation times, indicating that the difference in chain mobility must be related to the structural heterogeneity. In this section, the pulsed NMR analysis is used as well to investigate the heterogeneous structure of PVC/ClBz physical gels. Figure 9a shows the CPMG signals of the 5 g dL^{-1} PVC/ClBz gel at 30 °C. The decaying signals of PVC gels can be roughly decomposed into three exponential decaying components. First, the component *A* and *B* are the protons with the spin−spin relaxation time T_2 existing in the polymer-poor and polymer-rich phases, and the T_2^A and T_2^B values are about 1800 and 35 ms, respectively. The third Gaussian decaying component *C* with a very short T_2 value (ca. $T_2^C = 1.8$ ms) can be separated from the decaying signals. The samples begin to exhibit this hard component at $C > C^*_{gel}$. It is well-known that the molecular motion with the time scale of $T_2 \sim 0.01$ ms reflects a polymer crystal domain that has strong dipole interaction between the spins.[37] Actually, we cannot find any $T_2 \sim 0.01$ ms component in the PVC gels with the free induction decay (FID) analysis[38] in pulsed NMR measurement, although it is carried out using the solid echo pulsed sequence available for a short T_2 component, e.g., the crystalline domain in the gel system. Our previous study[2,4] also showed that the wide-angle X-ray diffraction curves for PVC gels could only present an amorphous scattering peak, indicating that the crystalline diffraction of microcrystals in gel network may be too small. Therefore, we suggest that the syndiotactic PVC sequences in the polymer-rich phase be associated with each other to act as order domain. Subsequently, the order domain and the denser aggregation of chain coils may construct a junction zone, leading to the formation of gel network. From the above consideration and the pulsed NMR results, the component *C* should be related to the molecular mobility of the protons in the junction zone, because the T_2 value (ca. 2 ms) is the time scale between the crystalline domain (ca. 0.01 ms) and polymer-rich phase (ca. 30 ms).

Figure 9b shows the T_2 values of three components which are separated from the CPMG decaying signals for PVC gels as a function of the $[\eta]C$ value at 30 °C. The component of the junction zone began to appear at $C > C^*_{gel}$, and the T_2^C values are almost independent of the concentration, indicating that the molecular mobilities of the protons in the junction zone are similar regardless of gelation conditions; i.e., the quality of the junction zone is the same. Figure 9b also shows that both the T_2^A and T_2^B values related respectively to the spin−spin relaxation time of polymer-poor and the polymer-rich phases decrease with concentration. This fact may be due to the initial spinodal decomposition. Because the phase separation of the solutions might not proceed fully into the equilibrium concentration of two coexisting phases, thus the concentration fluctuation of the spinodal decomposition process at the early stage is still observed. This result also indirectly confirms that the phase separation process of initial stage at the $1.5 < [\eta]C < 4$ region controls the morphology and makes a direct impact on the structure and properties of the gels.

Structural Characteristics of PVC Gels. By using the various scattering techniques Taleshita et al.[13,14] have proposed a good model for the hierarchic structure of PVA gel formed with the spinodal decomposition of the solution. However, our present study clarifies clearly the characteristics of various concentration regions and their influence on the structural formation of gels based on the spinodal decomposition process. This feature of PVC gelation is schematically illustrated in Figure 10a. In the concentration region of $[\eta]C > 1$, one can divide the gelation characteristics into four regions with increasing PVC concentration. (1) In the concentration region less than macroscopic percolation transition limit,[39] the polymer-rich phase transforms into isolated droplets, and the gelation cannot occur. (2) When the concentration is close to C^*_{gel} (ca. $[\eta]C = 1.5$), the gelation depends on the competition between the sol−gel and the dynamic percolation-to-cluster transitions; moreover, the structure and properties of gels are dominated by the evolution of the later-stage phase separation. (3) At the concentration between C^*_{gel} and C^* (ca. $[\eta]C \sim 4$), the phase separation of initial stage controls the structural formation and characteristics of gels. The result derived from this concentration region that agrees with our previous study for the gelation of PVDF/TG solution; i.e., the phase separation is the rate-determining step on gelation in the low-concentration

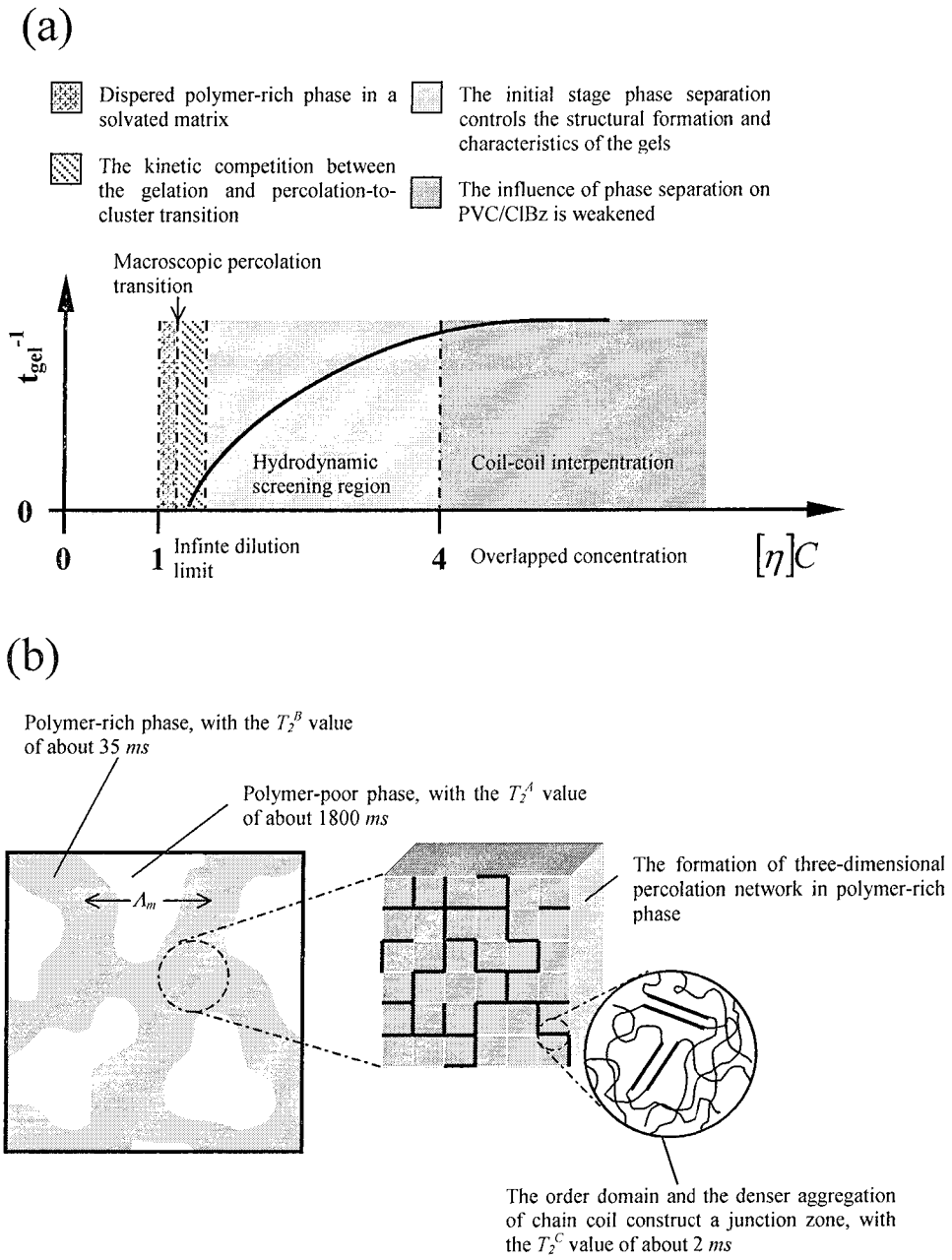

Figure 10. (a) Schematic picture for the effect of phase separation on structural formation of PVC/ClBz gelation at various concentration ranges. (b) Schematic model of hierarchic structure shows the effect of initial phase separation on gelation and the structural characteristic of gel at the concentration region of $1.5 < [\eta]C < 4$.

region.[5] (4) When the concentration is further increased more than $[\eta]C \sim 4$, the influence of phase separation on PVC/ClBz solution would be weakened due to the chain overlapping effect.

We now turn attention on region 3 to highlight the effect of initial phase separation on gelation. In our previous paper,[3] combining the dynamic light scattering and viscometric results, we have already proposed an aggregation mechanism for poly(vinyl chloride)/dioxane solution to explain the dynamic behavior of the solutions under phase separation. Similarly, the dynamic behaviors of PVC/DOA solutions could also be classified into three regions based on the $[\eta]C$ value. In the hydrodynamic screen region, i.e., $1 < [\eta]C < 4$, the relaxation time distribution was divided into two major relaxation modes; i.e., the fast mode is resembled as the individual PVC coil in the dilute solution, and the slow mode is related to the cluster formed from the aggregation of individual coils. When the PVC concentration is further increased, the third relaxation mode due to the transient gel network originated from the aggregation of clusters was observed. At the same time, the fast mode can still be found, and its diffusion coefficient has no remarkable change compared with that of individual chain coil in the dilute solution. With this we can conclude that the characteristics of intermolecular aggregation between the chain coils is the consequence of the initial spinodal decomposition in the semidilute region. Hence, the intermolecular association between chain coils, which occurs simultaneously in semidilute region with phase separation, is considered the most important feature during the gelation. It is possible to consider that the process of phase separation induces the aggregation of the chain coils in semidilute solutions. Then it would

increase the scattering level by concentration fluctuation. At the same time, the formation of a three-dimensional network structure should occur in the polymer-rich domain. If we consider that a chain coil occupies a lattice in a model of three-dimensional lattices, the gelation of percolation type could be suggested to describe the gelation behavior in the polymer-rich domain. Nevertheless, this concept is schematically illustrated in Figure 10b, and the process of gelation and the corresponding structural characteristics can be explained by a proposed model. One of the main characteristics of the spinodal decomposition at the early stage is to form the overall connected morphology, i.e., the spatially bicontinuous percolation structure, and since the phase separation process was restrained by macroscopic gelation, we can qualitatively explain the structural characterization of gels at the concentration region of $1.5 < [\eta]C < 4$ through the characteristic fluctuation wavelength, Λ_m. For a general idea of heterogeneous gelation, it would be expected that the intermolecular cross-linking occur only in the continuous polymer-rich phase because the polymer concentration in the polymer-poor phase is very diluted, especially for the present system. Hence, the contribution of the polymer-poor to gelation process may be neglected. Furthermore, we applied the concept of the percolation theory, which has been confirmed by an experiment on the gelation kinetics to interpret the structural formation of the three-dimensional network in the continuous polymer-rich phase. The centers of polymer coils occupy all sites of a three-dimensional periodic lattice, and then each bond between two nearest−nearest sites is formed randomly with probability. This concept would be rationalized when the gelation takes place near the chain-overlapped concentration due to the fact that the concentration fluctuation is relatively small at the early stage of spinodal decomposition, and it is approximately equal to the initial concentration. This approach has been used to reasonably demonstrate that the percolation-type association for polymer gelation is the consequence of intermolecular aggregation between chain coils in a phase separation process. Figure 10b also represents schematically the spin−spin relaxation times, T_2's, originating from polymer-rich, polymer-poor domains, and junction zone in gels.

Conclusion

The present study clarifies the characteristics of PVC solution at various concentration regions and their effect on the structural formation of gels with respect to the spinodal decomposition process. On the basis of the $[\eta]C$ value, one can divide the gelation characteristics into four regions according to their increasing PVC concentration. Furthermore, we confirmed that the percolation-type association for polymer gelation is the consequence of intermolecular aggregation between the chain coils during the initial stage of the phase separation process. A proposed model can explain this concept and its corresponding structural characteristics. However, it is necessary to mention that the gelation phenomenon has not been fully elucidated as the concentration nears the critical gelation concentration. Investigation of this critical gelation phenomenon requires further work including both theory and experimentation. To understand whether the critical gelation takes place in the phase separation region, we should clarify the two dynamical aspects. One of them is the sol−gel phase transition process, which may be dealt with a correlated percolation model, and the other is the dynamic percolation-to-cluster transition. The latter has been suggested that it may occur during the coarsening process of the spinodal decomposition. It may be expected that the gelation depends strongly on whether the dynamic percolation-to-cluster transition takes place or not. In general, the gelation does not occur once the percolated domain structure degenerates into isolated droplets.

Acknowledgment. The authors thank the National Science Council of the Republic of China for financially supporting this research under Contract NSC-89-2216-E-001-021.

References and Notes

(1) Hong, P. D.; Chen, J. H. *Polymer* **1999**, *40*, 4077.
(2) Hong, P. D.; Chen, J. H. *Polymer* **1998**, *39*, 711.
(3) Hong, P. D.; Chou, C. M.; Chen, J. H. *Polymer* **2000**, *41*, 5847.
(4) Hong, P. D.; Chen, J. H. *Polymer* **1998**, *39*, 5809.
(5) Hong, P. D.; Chou, C. M. *Polymer* **2000**, *41*, 8311.
(6) Banisil, R.; Lal, J.; Carvalho, B. L. *Polymer* **1992**, *33*, 2961.
(7) Matsuo, M.; Kawase, M.; Sugiura, Y.; Takematsu, S.; Hara, C. *Macromolecules* **1993**, *26*, 4461.
(8) Tanigami, T.; Suzuki, H.; Yamaura, K.; Matsuzawa, S. *Macromolecules* **1985**, *18*, 2595.
(9) Godard, J.; Biebuyck, J. J.; Dumerie, M.; Naveau, H.; Mercier, J. P. *J. Polym. Sci., Part B: Polym. Phys.* **1978**, *16*, 1817.
(10) Coniglio, A.; Stanley, H. E.; Klein, W. *Phys. Rev. Lett.* **1979**, *42*, 518.
(11) Staufer, D.; Coniglio, A.; Adam, M. *Adv. Polym. Sci.* **1982**, *44*, 103.
(12) Mal, S.; Maiti, P.; Nandi, K. *Macromolecules* **1995**, *28*, 2371.
(13) Takeshita, H.; Kanaya, T.; Kaji, K.; Nishida, K.; Nishikoji, Y.; Ohkura, M. *Kobunshi Ronbunshu* **1998**, *55*, 595.
(14) Takeshita, H.; Kanaya, T.; Nishida, K.; Kaji, K. *Macromolecules* **1999**, *32*, 7815.
(15) Hikmet, R. M.; Callister, S.; Keller, A. *Polymer* **1988**, *29*, 1378.
(16) Prasad, A.; Marand, H.; Madelkern, L. *J. Polym. Sci., Polym. Phys. Ed.* **1993**, *32*, 1819.
(17) Spering, L. H. *Introduction to Physical Polymer Science*; John Wiley & Sons: New York, 1986.
(18) Meiboom, S.; Gill, D. *Rev. Sci. Instrum.* **1958**, *29*, 688.
(19) Kaufman, S.; Slichter, W. P.; Davis, D. D. *J. Polym. Sci., Part A-2* **1971**, *9*, 829.
(20) Tank, H.; Nishi, T. *J. Chem. Phys.* **1986**, *85*, 6197.
(21) Dikshit, A. K.; Nandi, A. K. *Macromolecules* **1998**, *31*, 8886.
(22) Ohkura, M.; Kanaya, T.; Kaji, K. *Polymer* **1992**, *33*, 5044.
(23) Bohadanecky, M.; Kovar, J. *Viscosity of Polymer Solution*; Oxford: New York, 1982.
(24) Frish, H. L.; Simha, R. In *Reology Theory and Applications*; Eirich, F. R., Ed.; Academic Press: New York, 1956.
(25) Ohkura, M.; Kanaya, T.; Kaji, K. *Polymer* **1992**, *33*, 3686.
(26) Cahn, J. W.; Hilliad, J. H. *J. Chem. Phys.* **1958**, *28*, 258.
(27) Cahn, J. W. *J. Chem. Phys.* **1965**, *42*, 93.
(28) Hasegawa, H.; Shiwaku, T.; Nakai, A.; Hashimoto, T. In *Dynamics of Ordering Process in Condensed Matter*; Komura, S., Furukawa, H., Eds.; Plenum: New York, 1988.
(29) Van Aartsen, J. J. *Eur. Polym. J.* **1970**, *6*, 919.
(30) Debye, P. *J. Chem. Phys.* **1959**, *31*, 680.
(31) Debye, P.; Woermann, D. *J. Chem. Phys.* **1960**, *33*, 1746.
(32) Debye, P.; Woermann, D. *J. Chem. Phys.* **1962**, *36*, 1803.
(33) Ikehara, T.; Nishi, T.; Hayashi, T. *Polym. J.* **1996**, *28*, 169.
(34) Sugia, T.; Fukumopi, K.; Hirose, Y.; Okada, A.; Kurauchi, T. *J. Polym. Sci., Polym. Phys. Ed.* **1994**, *32*, 85.
(35) Tanaka, H.; Nishi, T. *Phys. Rev. B* **1986**, *33*, 32.
(36) Fukumori, K.; Kurauchi, T.; Kamigaito, O. *Polymer* **1990**, *31*, 713.
(37) Tanaka, H.; Nishi, T. *J. Chem. Phys.* **1985**, *82*, 4362.
(38) Powles, J. G.; Strange, J. H. *Proc. Phys. Soc.* **1963**, *82*, 6.
(39) Hayward, S.; Heermann, D. W.; Binder, K. *J. Stat. Phys.* **1987**, *49*, 1053.

MA0011439